Structure of the Cetyltrimethylammonium Surfactant at Fused Silica/Aqueous Interfaces Studied by Vibrational Sum Frequency Generation

Patrick L. Hayes, Alison R. Keeley, and Franz M. Geiger*

Department of Chemistry, Northwestern University, 2145 Sheridan Road, Evanston, Illinois 60208

Received: November 23, 2009; Revised Manuscript Received: January 25, 2010

Utilizing vibrational sum frequency generation (SFG), we characterized the structure of adsorbed cetyltrimethylammonium chloride (CTAC) at the silica/aqueous interface in the presence of 10 to 500 mM NaCl and as a function of surfactant surface coverage. For low ionic strengths (10 mM NaCl), results indicate that adsorbed aggregates do not change conformation with increasing surface coverage. Instead, the surfactant adsorbs as micelle-like structures at concentrations considerably lower than surface saturation and the CMC. At high ionic strengths (300−500 mM NaCl), the structure of the adlayer is considerably different: The SFG results indicate that for 30 μM bulk CTAC the surfactant packs with fewer *gauche* defects in the hydrocarbon backbone, which is attributed to reduced Coulomb repulsion between the positively charged surfactant headgroups, and the results also indicate that CTAC adsorbs as monomers at low surface coverage but then rearranges into aggregates at higher surface coverage.

I. Introduction

Surfactant adsorption to solid/aqueous interfaces is an important chemical process that impacts a variety of technologies ranging from nanoparticle synthesis to fracturing fluids for enhanced oil recovery.[1,2] It is not surprising then that this subject has been studied extensively, and several excellent reviews on the interaction of surfactants with solid/aqueous interfaces are available in the literature.[3,4] The work presented here addresses the common cationic surfactant, cetyltrimethylammonium (CTA), at the equally common hydrophilic fused silica surface. We utilize vibrational sum frequency generation (SFG) to probe the ordering of adsorbed cetyltrimethylammonium (CTA) at the silica/aqueous interface for a variety of bulk concentrations including those significantly lower than the CMC (∼10%). Characterizing the structure of adsorbed surfactants at low surface coverage is a significant scientific challenge. However, using SFG, we are able to probe CTA structure at both high and low surface coverage and, thereby, demonstrate that SFG complements other techniques such as AFM, which have been used to probe surfactant structure at high surface coverage. Specifically, our SFG results constrain the morphologies that could plausibly be assumed by CTA at the silica/aqueous interface for pH 11 and a range of ionic strength conditions (10−500 mM NaCl).

One advantage of studying CTA is that its adsorption to SiO_2/aqueous interfaces has been extensively characterized by a variety of techniques. Previous studies have utilized bulk depletion measurements,[5] optical reflectometry (OR),[6,7] ellipsometry,[8] atomic force microscopy (AFM),[6,9] quartz crystal microbalances (QCMs),[7,10,11] neutron reflection,[12] SFG,[13] and total internal reflection Raman scattering.[13] This work has provided much needed information on the thermodynamics, kinetics, nanometer-scale morphology, and the molecular-level conformation of CTA at the SiO_2/aqueous interface.

Despite the breadth of this previous research, there are few studies of quaternary alkyl ammonium surfactant adsorption at high ionic strengths (i.e., more 10 mM added salt), even though important technological applications require such surfactant/salt mixtures.[1] To address this knowledge gap our group recently reported second harmonic generation (SHG) and SFG studies of CTA adsorption at the silica/aqueous interface in the presence of 10, 100, 300, and 500 mM concentrations of NaCl.[14] From the SHG adsorption isotherms free energies of adsorption at each salt concentration were calculated. By analyzing the free energies as a function of interfacial potential, we determined that CTA adsorption is primarily driven by the favorable hydrophobic interactions between surfactant hydrocarbon chains, and we quantified the extent of counterion coadsorption with CTA. Furthermore, utilizing SFG we recorded the vibrational spectrum of adsorbed CTA in the C−H stretching region and assigned the observed resonances using deuterium substitution studies.

Building on this previous work, we report here new SFG studies across a much broader range of surfactant concentrations (15−700 μM) and NaCl concentrations (10−500 mM). This expanded approach provides fundamental insight into how the structure of the surfactant adlayer changes with varying ionic strength and CTA surface coverage. Additionally, the SFG experiments are focused on the C−H stretching region of the spectrum, which partially overlaps with the O−H resonance of water. Thus, changes in the ordering of water at the silica surface in the presence of salt and adsorbed surfactant can be tracked. Following our previous procedures, all experiments were carried out a pH 11, which was selected because it provides improved signal-to-noise for the SHG experiments and possibly for the SFG experiments as well.

Given the sensitivity of sum frequency generation spectroscopy to the orientation and ordering of adsorbed species, it is a potentially powerful technique for probing the structure of adsorbed surfactant monomers and aggregates. Within the electric dipole approximation, adsorbates that organize into centrosymmetric macromolecular structures should exhibit no SFG spectra due to the net cancellation of contributions to the signal from oppositely oriented resonant transitions. This principle holds for all second-order optical processes.[15,16] In

* To whom correspondence should be addressed. E-mail: geigerf@chem.northwestern.edu.

10.1021/jp911116q
Published on Web 03/11/2010

actuality, centrosymmetric structures may yield second-order responses due to defects or external perturbations, such as static electric fields, that break the symmetry of the system. Nevertheless, strong decreases in the SFG signal intensity are often observed for changes in molecular conformation wherein a noncentrosymmetric structure rearranges into a centrosymmetric one as beautifully demonstrated by the Conboy, Richmond, and Walker groups.[17−19] Rearrangement of surfactants from a monolayer into a bilayer or from ordered monomers into micelles adsorbed at interfaces should therefore be observable in SFG spectra as a decrease in signal intensity.

II. Cetyltrimethylammonium Cations at Solid/Aqueous Interfaces: The Influence of Counter Ions and Ionic Strength

When adsorbed to the silica/aqueous interface CTA may form aggregates, which can adopt "worm-like" or round "micelle" morphologies depending on the identity of the counterions and the concentration of surfactant. The influence of these factors on morphology was demonstrated in AFM experiments reported by Velogol and co-workers.[6] At high concentrations (10× CMC), cetyltrimethylammonium bromide (CTAB) was found to form "worm-like" micelles at the silica/aqueous interface in the absence of added electrolyte and also in the presence of 10 mM KBr. At lower concentrations (0.9× CMC), short rods and spheres were observed in both the absence and presence of 10 mM KBr. When cetyltrimethylammonium chloride (CTAC) was studied under analogous conditions only spheres were observed. In contrast, Hodges et al. reported that at ∼6 mM CTAC concentrations adsorbed surfactant formed "worm-like" adsorbed aggregates in the presence of 3−4 M NaCl,[9] which suggests that sufficiently high chloride concentrations can drive changes in aggregate morphology.

The important role that counterions play in CTA adsorption is not surprising given their well-known influence on micelle structure[3,20] and importance in electrical double-layer models.[21,22] Counterion binding in bulk CTA micelles and its impact on bulk micelle shape has been quantitatively characterized for a variety of systems.[20,23] There is also significant experimental work examining the influence of electrolyte on surfactant adsorption, and early research in this area mostly relied on depletion and ζ-potential measurements.[4] More recently, though, AFM studies and optical reflectometry studies[7,24] have provided new information regarding kinetics, structure and the impact of ionic strength on these properties. This work has addressed CTA adsorption at the silica/water interface, and specifically, AFM measurements have provided valuable information about the morphology of the adsorbed surfactant in the presence of added electrolyte,[6,9] which is described in the preceding paragraph. However, with one exception,[25] adlayer structure has been investigated using AFM only for bulk surfactant concentrations corresponding to complete or near surface saturation (i.e., 100 mM or higher for circum-neutral pH values). Here, we extend this lower limit using SFG and probe adlayer structure in the presence of NaCl at surfactant concentrations lower than those studied previously by AFM.

III. Sum Frequency Generation

The theoretical and experimental details of SFG have been described previously,[26−29] and thus, only a short summary will be provided. In a noncentrosymmetric medium, such as an interface, two electric fields (E-fields) will couple and produce a third SFG E-field at a frequency equal to the sum of incident frequencies without contribution from the centrosymmetric bulk phases. When an incident field frequency matches a vibrational or electronic resonance in an interfacial species, the SFG signal is resonantly enhanced. In general, SFG spectra are acquired by monitoring the SFG signal across a range of incident IR wavelengths while holding the frequency of the second, visible field constant. As shown in eq 1, the intensity of the SFG signal, I_{SFG}, is proportional to the square modulus of the second-order susceptibility of the interface, $\chi^{(2)}$, and the intensity of the input visible, I_{vis}, and IR, I_{IR}, light fields.

$$I_{SFG} \propto |\chi^{(2)}|^2 I_{vis} I_{IR} \tag{1}$$

The second-order susceptibility can be expressed as the sum of nonresonant and resonant contributions, $\chi_{NR}^{(2)}$ and $\chi_{R\nu}^{(2)}$, respectively (eq 2).

$$I_{SFG} \propto |\chi_{NR}^{(2)} e^{i\gamma_{NR}} + \sum_{\nu=1}^{n} \chi_{R\nu}^{(2)} e^{i\gamma_\nu}|^2 I_{vis} I_{IR} \tag{2}$$

In eq 2, the resonant contribution is summed over all vibrational modes, ν, and γ represents the phase factors associated with both the nonresonant background and the vibrational modes. The resonant contribution can then be modeled as the product of the number of resonating surface-bound molecules, N_{ads}, and the molecular hyperpolarizability, β_ν, averaged over all orientations of the molecules (eq 3).

$$\chi_{R\nu}^{(2)} = N_{ads} \langle \beta_\nu \rangle \tag{3}$$

The value of β_ν increases when the frequency of the incoming IR pulse matches a vibrational transition of an interfacial species leading to resonance enhancement of the SFG signal. As suggested in eq 3, the ordering and orientation of adsorbates within the interfacial region determine SFG spectral peak intensities and polarization dependence.[13,30−32]

The absolute CTA surface coverage was evaluated and quantified in our previous work,[14] where we tracked surfactant binding at the silica/aqueous interface by utilizing the Eisenthal $\chi^{(3)}$ technique. This technique has also been used to quantify the thermodynamics and electrostatics of metal cation[33−35] and protein adsorption,[36] as well as DNA-functionalized surfaces[37,38] and acid−base equilibria.[33,39,40] For a description of how SHG can be used to determine relative surfactant surface coverage, please see the Supporting Information.

IV. Experimental Methods

A. Broadband SFG System. Our setup for the SFG experiments has been described in detail previously.[14] Thus, only a brief description of the laser system and optical configuration that is pictured in Figure 1 will be provided. Laser light (800 nm, ∼120 fs pulses, 1 kHz repetition rate) from a regeneratively amplified Ti:Sapphire laser system (Spitfire Pro, Spectra Physics) is passed through a 50/50 beam splitter, and half of the beam is used to pump an optical parametric amplifier (OPA-800CF, difference-frequency mixing option, Spectra Physics) to produce broadband (∼140 cm^{-1} fwhm) IR laser light at a wavelength around 3.4 μm. This IR beam is then focused on the fused silica/aqueous interface using a BaF_2 lens (ISP Optics). The remaining half of the original laser beam passes through a home-built time delay stage to control timing and a narrow bandpass filter (F1.1-800.0-UNBLK-1.00, CVI Melles Griot) to

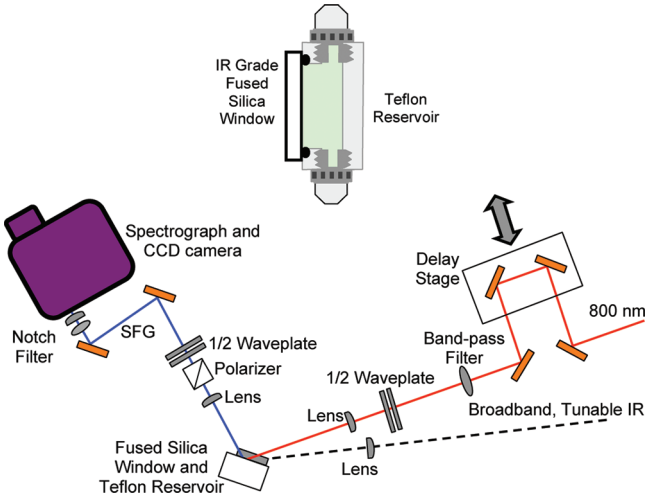

Figure 1. The experimental setup and liquid reservoir used in the SFG experiments. See experimental methods section for further details. Top inset: Side view of the liquid reservoir used for the CTAC/NaCl solutions. The outlet and inlet point down and up, respectively, along an axis perpendicular to the laser table. Bottom: overhead view of the SFG setup. Reflected 800 nm and IR beams are omitted for clarity.

provide spectrally narrow 800 nm pulses. An achromatic half-waveplate (MWPAA2-12-700-1000, Karl Lambrecht Corp.) allows for polarization rotation of the 800 nm laser light. The 800 nm and IR beams are focused on to the interface at angles of 45 and 60° from normal, respectively. When measured in-line immediately before the sample, typical pulse energies for the visible and IR beams are 4 and 2 μJ, respectively. The polarization of the SFG signal generated from the sample is selected by a polarizer (Glan Laser Polarizer, GL15, Thorlabs) after which a half-waveplate (MWPAA2-12-400-700, Karl Lambrecht Corp.) rotates the SFG polarization for optimal throughput to the detector. Then the SFG signal passes through a long-pass filter (600 nm cutoff) to remove light from nonlinear processes other than SFG and an 800 nm notch filter (Notch Plus Filter, Kaiser Optical Systems, Inc.) to remove reflected 800 nm light. A spectrograph (Acton Research) coupled to a liquid nitrogen cooled, back-thinned, charged coupled device camera (Roper Scientific, 1340 × 100 pixels) is used for signal detection.

The frequency axes for the sample SFG spectra are calibrated by measuring the SFG spectrum of a PMMA standard. For this procedure, the C−H symmetric stretch of the methoxy group in poly(methyl) methacrylate (PMMA) is used as a single calibration point at 2955 cm^{-1} (after subtracting out the frequency of the 800 nm beam).[41] Thin films of PMMA were spin-coated onto an IR grade fused silica window according to our published procedure,[42,43] and after each experiment a PMMA SFG spectrum was collected at the fused silica/air interface with the same experimental geometry and alignment as used for the CTAC studies (i.e., reflection geometry). Background subtraction is performed using spectra acquired after blocking the IR input, thus accounting for optical scatter from the 800 nm beam. To account for the line shape of the incident broadband IR pulse, all SFG spectra are normalized to the nonresonant SFG spectrum of a gold-coated IR grade fused silica window following the method of Esenturk and Walker.[30]

B. Materials and Sample Cells. All SFG experiments were performed using a custom-built chamber consisting of a fused silica window (ISP Optics, IR grade) clamped upon the open top of a Teflon reservoir (Figure 1, inset). A Viton O-ring, cleaned twice daily before and after experiments with Millipore water (18.2 MΩ), was used to seal the window to the reservoir without leakage. Aqueous solutions of CTAC (Sigma-Aldrich, 98%) and NaCl (VWR, 99%) were prepared using Millipore water or D_2O (Cambridge Isotope Laboratories, 99.9 atom % D), and the solutions were adjusted to a pH or pD of 11.0 (±0.1) with NaOH (Fisher, 98.8%) and NaOD (Alfa Aesar, 40% w/w solution in D_2O, 99.5 atom % D) solutions. All chemicals were used as received. Prior to each experiment, the fused silica window was cleaned by rinsing with methanol and sonication in methanol for 6 min. The substrate was then dried in a 100 °C oven for ~30 min and subjected ~45 s of plasma cleaning in 500−1000 mTorr of air. Following plasma cleaning, the window was immediately placed atop the Teflon flow cell or stored under vacuum for up to ~6 h.

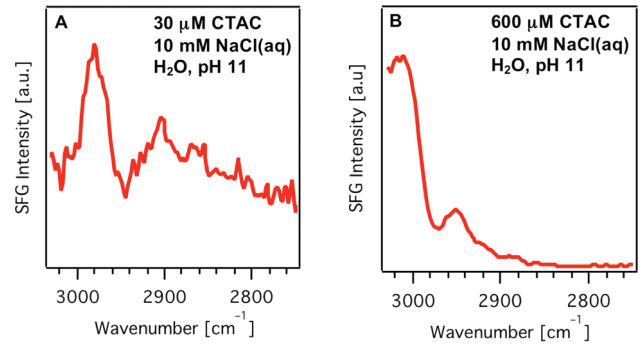

Figure 2. ssp-Polarized SFG spectra obtained from the fused silica/H_2O interface at pH 11 for (A) 30 μM CTAC and (B) 600 μM CTAC. All spectra were collected in the presence of 10 mM NaCl(aq).

C. Contact Angle and Interfacial Tension Measurements. A First Ten Ångstroms (FTÅ 125) goniometer was used to measure interfacial tensions (IFT) via the pendant drop method,[44] as well as sessile contact angles on glass slides (Fisher Scientific, Catalog Number: 12-544-5CY). The IFT measurements were utilized to calculate CMC concentrations of 2.2(2) × 10^{-4}, 1.8(2) × 10^{-4}, 2.1(2) × 10^{-4}, and 2.2(2) × 10^{-4} M for CTAC in the presence of pH 11 and NaCl concentrations of 10, 100, 300, and 500 mM, respectively. Please see the Supporting Information for details of CMC measurements.

V. Results and Discussion

A. Vibrational Sum Frequency Generation Spectra. Following Esenturk and Walker's procedure[30] as well as our own previously published procedure,[14,43] broadband SFG spectra were recorded with four different input IR center frequencies and then summed to provide an SFG spectrum in the entire C−H stretching region. Aqueous CTAC solutions were introduced into the reservoir by pipet and allowed to equilibrate for 20 min. This waiting period was selected based on equilibration times observed in time-resolved SFG and SHG adsorption experiments.[14] Longer time-scale adsorption may occur in our system,[7] but it is not detectable within the signal-to-noise limits of our techniques and over the time scales of our experiments (~30 min).

Figure 2 shows ssp-polarized SFG spectra obtained from the silica/aqueous interface for low (30 μM, panel A) and high (600 μM, panel B) bulk CTAC concentrations in the presence of 10 mM NaCl. The notation "ssp" refers to the polarization of the incident and exigent beams where the first letter refers to the polarization of SFG light (s-polarized), the second refers to the polarization of 800 nm light (s-polarized), and the third refers to the polarization of the IR light (p-polarized). All spectra reported here were collected using the ssp polarization combina-

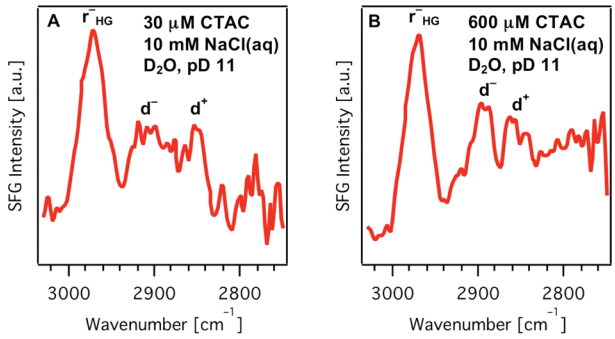

Figure 3. ssp-Polarized SFG spectra obtained from the fused silica/D_2O interface at pD 11 for (A) 30 μM CTAC and (B) 600 μM CTAC. All spectra were collected in the presence of 10 mM NaCl(aq).

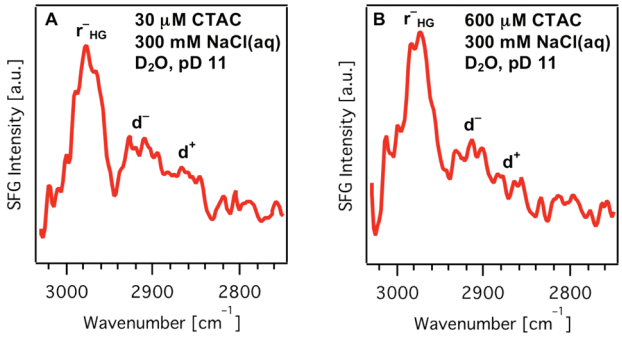

Figure 4. ssp-Polarized SFG spectra obtained from the fused silica/D_2O interface at pD 11 for (A) 30 μM CTAC and (B) 600 μM CTAC. All spectra were collected in the presence of 300 mM NaCl(aq).

tion, which samples the component of the vibrational transition dipole moment that is aligned along the surface normal.[30] This polarization combination was chosen because it provided the greatest signal-to-noise in the acquired spectra. Alternatively, ppp- and sps-polarized spectra were collected (data not shown), but their poor signal-to-noise limits spectral analysis. It should be noted that the spectra displayed in Figures 2−4 were collected over several days using acquisition times ranging between 1 and 2 h per spectrum. Direct comparisons of peak intensities between the different spectra are therefore not possible, although comparisons of peak ratios are possible (vide infra). Due to these considerations, the panels in Figures 2−4 are scaled to each individual spectrum for clarity. The SFG spectrum in Figure 2A clearly shows a peak at 2975 cm^{-1}, which was assigned in our previous work via deuteration studies[14] to the asymmetric methyl stretch of the ammonium headgroup. The sloping baseline also observed in Figure 2A is attributable to water OH stretching modes, which generally produce broad features in vibrational SFG spectra that exhibit a lower energy peak centered at roughly 3200 cm^{-1}.[13,45]

The spectrum corresponding to high CTAC concentrations in Figure 2B is more challenging to interpret. The derivative line shape probably results from interference[46] between the C−H and water resonances. The dramatically higher contribution to the SFG signal from water relative to the C−H modes is explained by the net positive charge at the silica/aqueous interface resulting from adsorbed CTAC, which leads to a long-range array of aligned water dipoles that gives rise to a stronger resonant water signal than is observed in the low concentration spectrum (Figure 2A).[13]

The interpretation of the CTAC SFG spectra is greatly simplified by carrying out experiments in D_2O under equivalent conditions as used in the H_2O work (i.e., 10 mM NaCl and pD 11, with pD adjusted using NaOD). In Figure 3, three C−H resonances are evident at low surfactant concentrations (30 μM). The major, well-resolved peaks can be assigned to asymmetric stretch of the ammonium methyl groups at 2975 cm^{-1} (r^-_{HG}), the asymmetric methylene stretch at 2919 cm^{-1} (d^-), and the symmetric methylene stretch at 2856 cm^{-1} (d^+). The two methylene modes correspond to the surfactant hydrocarbon backbone[14] and are more clearly resolved in the D_2O spectrum. The three C−H peaks are also present in the SFG spectrum at high surfactant concentrations (600 μM), although they now overlap with the shoulder of the D_2O stretching resonance that is shifted to ~2400 cm^{-1} due to deuteration.[47]

To explore the influence of ionic strength on the SFG spectra, experiments were also carried out for the silica/aqueous interface in the presence of 300 mM NaCl with low (30 μM) and high (600 μM) surfactant concentrations. The spectra are displayed in Figure 4A and B, respectively. Interestingly, the shoulder of the O−D stretch for D_2O is not observed even at the high surfactant concentrations. The absence of a contribution from D_2O in the SFG spectrum indicates that there is little net orientation of water molecules at the fused silica/aqueous interface under the experimental conditions.

In recent work, Jena and Hore[48] demonstrated that increasing ionic strength diminished the magnitude of the SFG spectrum of water at the silica/water interface (pH ~6.5), although water resonances were still observed up to the maximum ionic strength studied (120 mM NaCl). Additionally, Tyrode et al. showed that, at pH 5.6 and in the absence of added electrolyte, adsorbed CTAB might dramatically increase or decrease the magnitude of the water contribution to the SFG spectra depending on the bulk surfactant concentration.[13] However, in this latter work, a complete disappearance of the water O−H stretching mode was only observed at a specific surfactant concentration corresponding to a net neutral surface charge. In contrast, the SFG spectra presented in Figure 4 display no water O−D resonances across a broad range of CTAC concentrations, which suggests that adsorbed surfactant in the presence of high ionic strengths (i.e., hundreds of mM salt concentrations) disrupts water structure at fused silica/aqueous interfaces with a bulk of pH 11.

B. Ionic Strength and Surfactant Aggregate Ordering. In addition to the changes in the water resonances, another difference between the low ionic strength and high ionic strength spectra is the relative C−H peak intensities. This difference is clearest between the spectra displayed in Figure 3A and Figure 4A, because there is minimal convolution of the C−H peaks with the D_2O resonances. The SFG spectra show that the peak intensities for the symmetric (d^+) and asymmetric (d^-) stretches of the methylene groups become weaker relative to the asymmetric stretch of the ammonium methyl groups (r^-_{HG}) as the ionic strength increases. Specifically, for the low ionic strength spectrum (10 mM NaCl), an intensity ratio of 0.5 is calculated for the asymmetric methyl stretch at 2975 cm^{-1} and the symmetric methylene stretch mode at 2856 cm^{-1} (d^+/r^-_{HG}), while a ratio of 0.3 is calculated for the high ionic strength spectrum (300 mM NaCl).

To test the generality of this observation, we calculated the values of d^-/r^-_{HG} and d^+/r^-_{HG} from SFG spectra recorded at 10, 300, and 500 mM NaCl and 30 μM CTAC concentrations. The results are summarized in Figure 5, which shows that these ratios decrease with increasing NaCl concentration. The SFG intensity was calculated by taking the average of several points spanning each peak maximum by 7 cm^{-1}. This simple treatment of the SFG spectra requires the nonresonant and resonant water contributions to the SFG spectra to be negligible. Given the spectra displayed in Figure 3A and Figure 4A and the concen-

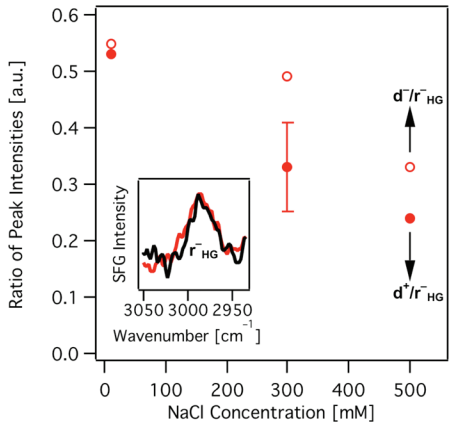

Figure 5. Ratio of the methylene symmetric (solid circles) and methylene asymmetric (hollow circles) to the asymmetric methyl mode intensities calculated from the SFG spectra at varying NaCl concentrations. The methylene modes correspond to the hydrocarbon backbone of CTAC and the methyl mode corresponds to the ammonium headgroup. The decrease in the ratio with increasing NaCl concentrations is indicative of conformational changes occurring within the adlayer. See text for further details. Inset: ssp-Polarized SFG spectra of the ammonium methyl asymmetric stretch of CTAC (30 μM) for 10 mM (red trace) and 300 mM (black trace) NaCl concentrations.

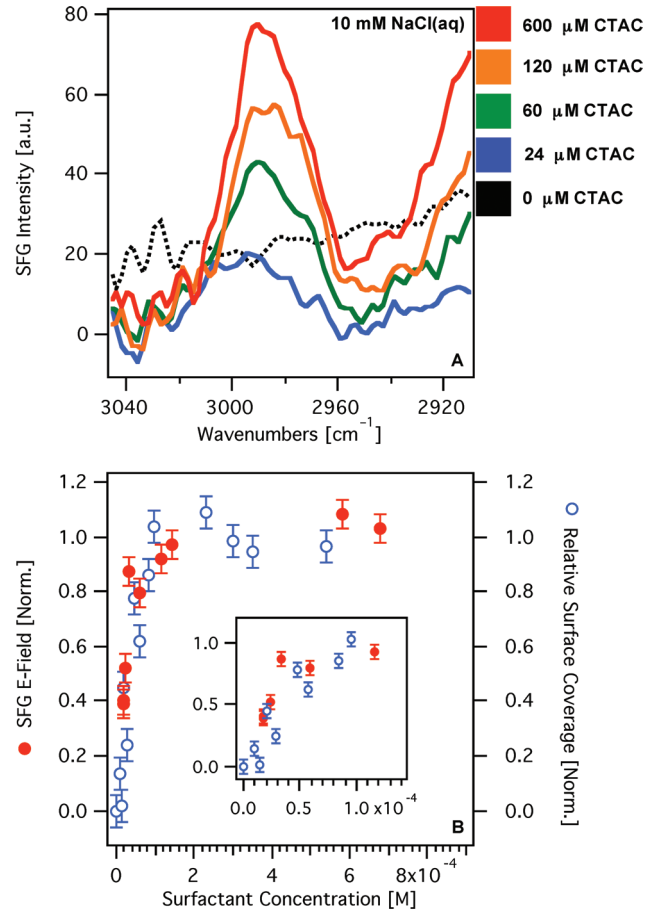

Figure 6. (A) ssp-Polarized SFG spectra obtained from the fused silica/D_2O interface at pD 11 in the presence of 10 mM NaCl(aq). Colored traces correspond to the following concentrations of CTAC: 0 (black, dotted), 24 (blue), 60 (green), 120 (orange), and 600 μM (red). (B) The normalized, resonant SFG E-field magnitude (red solid circles, left axis) corresponding to the asymmetric methyl stretch of the ammonium headgroup plotted as a function of surfactant concentration. For comparison, the normalized surface coverage of adsorbed surfactant (blue hollow circles, right axis), as determined by previously published SHG experiments,[14] is plotted with the SFG data. See text for further explanation regarding determination of the resonant SFG E-field magnitude and the surfactant surface coverage. Inset: Expanded view of the low concentration data.

tration dependent studies displayed in Figure 6A and Figure 7A (vide infra), this requirement appears to be satisfied for surfactant concentrations near 30 μM where the SFG contribution from water is negligible across the range of ionic strengths studied. Our calculations also ignore possible interference between different C−H resonances. To partly account for this possibility, we calculated intensity ratios for the asymmetric and symmetric methylene modes, which follow the same decreasing trend. This finding suggests that interference between different modes can be partly accounted for with this method of double ratios.

The decreasing trend in the d^-/r^-_{HG} and d^+/r^-_{HG} intensity ratios can be interpreted by considering the local symmetry and orientation of the methylene groups in the hydrocarbon backbone. An all-*trans* hydrocarbon chain is locally centrosymmetric with respect to the methylene groups, and those groups are therefore symmetry forbidden in SFG.[18,19] While this reasoning applies rigorously only to an all-*trans* symmetric alkane molecule having an even number of methylene groups, several reports have shown that increased conformational ordering reduces the methylene response regardless of chain length or molecular identity.[19,32] The methylene vibrations will become SFG active when a *gauche* defect breaks the local symmetry along the hydrocarbon backbone. These symmetry arguments do not apply to the methyl groups, and thus, a lower d^+/r^-_{HG} and d^-/r^-_{HG} ratio would be consistent with greater conformational ordering (i.e., less *gauche* defects) in the surfactant hydrocarbon backbone. From Figure 5, it then follows that increasing the ionic strength of the system reduces the number of *gauche* defects and drives ordering within the hydrophobic region of the surfactant adlayer.

There are alternative explanations for the decrease observed in the intensity ratios. An increase in the methyl asymmetric mode intensity due to rearrangement of the surfactant headgroups could lead to a decrease in the ratios. To rule out this possibility, SFG spectra of the methyl asymmetric mode were collected for low (10 mM) and high (300 mM) NaCl concentrations in consecutive experiments, while carefully monitoring input laser power. In the raw (i.e., not scaled) SFG spectra shown in the Figure 5 inset, it can be clearly seen that there is no change in the methyl asymmetric mode intensity with ionic strength, which indicates that the decreasing trend for the intensity ratios is directly attributable to the lower intensity of the methylene modes at higher ionic strength. The decreasing intensity of the d^+ and d^- modes could possibly arise from the adsorbed surfactant hydrocarbon chains rearranging into a more symmetric macromolecular structure. This scenario cannot be ruled out using the SFG data alone. However, the work of Subramanian et al. showed that CTAC adsorbed aggregates in the presence of 250 mM LiCl retained the same spherical morphology as observed in the analogous system without added salt.[49] The lack of rearrangement at these high chloride concentrations is consistent with other reports that indicate chloride binding to surfactant aggregates is weak in comparison to bromide.[50] Therefore, it seems likely that the decrease in the intensity ratios is attributable to a decrease in gauche defects within adsorbed micelle aggregates rather than a rearrangement of the aggregate structure. Regardless of the exact molecular origin of the decreasing intensity ratios, clearly a significant rearrangement is occurring within the adlayer with increasing NaCl.

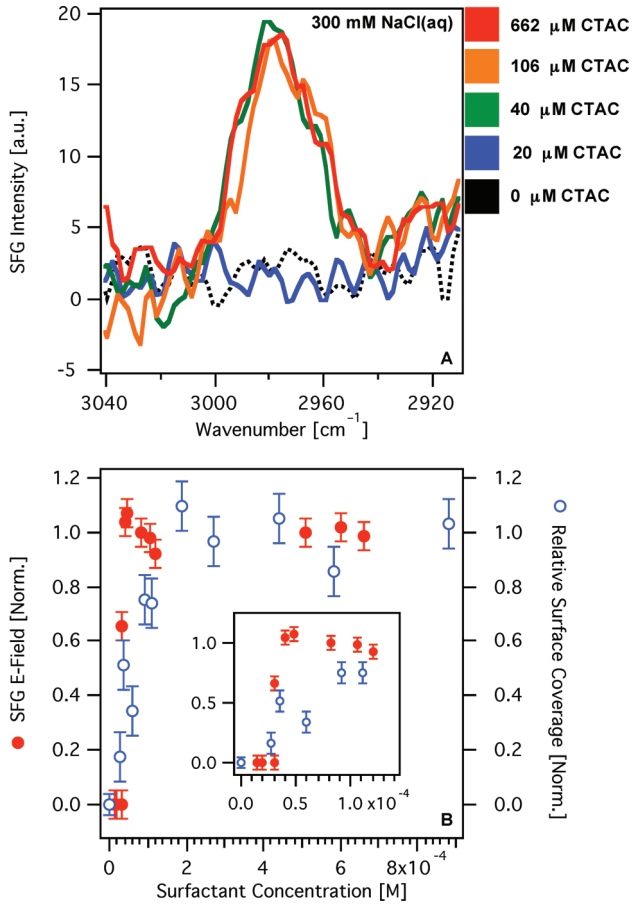

Figure 7. (A) ssp-Polarized SFG spectra obtained from the fused silica/D_2O interface at pD 11 in the presence of 300 mM NaCl(aq). Colored traces correspond to the following concentrations of CTAC: 0 (black, dotted), 20 (blue), 40 (green), 106 (orange), and 662 μM (red). (B) The normalized, resonant SFG E-field magnitude (red solid circles, left axis) corresponding to the asymmetric methyl stretch of the ammonium headgroup plotted as a function of surfactant concentration. For comparison, the normalized surface coverage of adsorbed surfactant (blue hollow circles, right axis), as determined by previously published SHG experiments,[14] is plotted with the SFG data. See text for further explanation regarding determination of the resonant SFG E-field magnitude and the surfactant surface coverage. Inset: Expanded view of the low concentration data.

One explanation for the rearrangement focuses on the role of counterions, which can bind to the charged surfaces of micelles and adsorbed aggregates and decrease Coulombic repulsion between the headgroups.[14,23] If Coulombic repulsion decreases with increasing ionic strengths, then the surface area per headgroup would be reduced at high NaCl concentrations,[51] which would force the hydrocarbon chains to pack more efficiently. The more tightly packed aggregates would then be expected to have less *gauche* defects or higher aggregate symmetry and, thus, lower SFG intensity ratios, as observed in Figure 5. This conclusion is consistent with optical reflectometry experiments that show a significant increase in the adsorbed CTAC surface density in the presence of 10 mM KCl versus the same system with no added electrolyte.[6] Here, we demonstrate this effect for salt concentrations up to 500 mM.

C. Surface Coverage and Surfactant Aggregate Structure: Low Ionic Strength. To explore how ionic strength *and surface coverage* combine to control adlayer structure at the silica/aqueous interface, SFG spectra were collected at 10 and 300 mM NaCl at CTAC concentrations corresponding to varying degrees of surface coverage. For these studies, the IR laser center frequency was tuned to match the resonant frequency of the asymmetric methyl stretch of the ammonium headgroup at 2975 cm^{-1}, and successively increasing concentrations of surfactant were introduced into the SFG sample cell. Given the frequency bandwidth of the IR laser (~140 cm^{-1} fwhm), all of the vibrational resonances in CTAC cannot be studied simultaneously, and tuning the laser source for each surfactant concentration to acquire a full spectrum of the C−H stretching region is prohibitively time-consuming. Thus, we choose to focus on the methyl asymmetric stretch, which provides the highest signal-to-noise. It also should be noted that discrepancies are observed in measurements of surfactant surface excesses when different sample introduction procedures are used. For instance, experiments where bulk concentrations are *increased* in a stepwise fashion yield systematically lower surface excesses than experiments where concentrations are *decreased*.[10,11] Therefore, we utilized sequential addition for this work because it allows for better comparison to previously published results.[6,11,13]

For 10 mM NaCl and in the absence of surfactant, the SFG spectrum displays a slight sloping baseline due to the shoulder of the D_2O vibrational resonance (Figure 6A). At 24 μM CTAC, the shoulder is much weaker, while the methyl asymmetric stretch is already visible in the spectrum at this relatively low surface coverage (~40% of a surface saturation). As depicted in Figure 6A, the resonance grows in intensity with higher surfactant concentrations, and simultaneously, a shoulder appears at lower wavenumbers. This shoulder is attributable to a combination of the D_2O resonance and also the methylene asymmetric and symmetric stretches discussed earlier in this work.

Above 3020 cm^{-1}, the D_2O and C−H resonances do not contribute significantly to the SFG spectra, and there is little change in the SFG spectra baselines with increasing surfactant concentration from 24 μM to 600 μM. This observation indicates that the nonresonant contribution to the SFG spectra is negligible. The nonresonant response can be reasonably treated as an IR frequency independent constant.[52] From previous SHG experiments carried out in our group,[14] the nonresonant signal should decrease when increasing surfactant concentration from 24 to 600 μM due to progressively more positive surface charging. However, it is clearly observed above 3020 cm^{-1} that the baseline remains constant, indicating that nonresonant contributions to the SFG spectrum are small in magnitude compared to the resonant contributions. This conclusion rectifies our previous report[14] in which we identified large changes in the SFG baseline intensity above 3020 cm^{-1} observed during surfactant adsorption as nonresonant signal contributions. Given the new data presented here, this large change in baseline was most likely due to the shoulder of the water O−H vibrational resonance, which is avoided here through use of D_2O.

To quantify the concentration-dependent increase in the asymmetric methyl stretch, we plotted the magnitude of the SFG E-field for this peak against the bulk CTAC concentration (Figure 6B, solid red circles). For comparison, the relative surfactant surface coverage as determined previously from our SHG studies[14] is plotted as empty blue circles on the same figure and scale as the SFG data. The SFG E-field magnitudes were calculated by taking the square root of the peak intensities, which were determined using the procedure described in the previous section.

When comparing the SFG and surface coverage data in Figure 6B, it is apparent that the SFG data increases in-step with surface coverage within the precision of our measurements. This match leads us to conclude that changes in average orientation do not

influence the SFG E-field as surface coverage is increased. The SFG E-field is increasing solely due to an increase in the number of adsorbates. This finding indicates that increasing the surfactant surface coverage is not associated with major changes in the CTAC orientation. Molecular rearrangement such as from a monolayer to a bilayer would cause a decrease in the SFG E-field due to increasing symmetry of the adlayer and partial cancellation of the oppositely oriented transition dipoles.[13] AFM experiments by Velegol et al. have shown that CTAC in the presence of 10 mM KCl adsorbs to the silica/aqueous interface as spherical structures, presumably adsorbed micelles, at concentrations near surface saturation and higher (pH $\sim$ 5.6). These results combined with the evidence from our SHG and SFG experiments that major rearrangement does not occur implies that CTAC adsorbs to silica as spherical structures at 10 mM NaCl and surfactant concentrations as low as 17 μM, which corresponds to only $\sim$40% of surface saturation and is significantly below the CMC (220 μM).

D. Surface Coverage and Surfactant Aggregate Structure: High Ionic Strength. To test for differences in adsorption at higher ionic strengths, SFG spectra were collected at 300 mM NaCl across the same range of CTAC concentrations as used for the 10 mM NaCl experiments (Figure 7A). Using these spectra, the SFG E-fields for the asymmetric methyl stretch and the relative surface coverage[14] are plotted together (Figure 7B). A significant change is observed in the SFG data for the two ionic strengths when comparing Figures 6B and 7B. While the 10 mM NaCl system (Figure 6B) displays an increase in SFG E-field that follows surface coverage, the 300 mM NaCl system (Figure 7B) follows a step function. With the 10 mM NaCl system, the asymmetric methyl stretch is clearly observed at CTAC concentrations as low as 17 μM, whereas for the 300 mM NaCl system the asymmetric methyl stretch is not observed for bulk CTAC concentrations up to 30 μM. Starting at 30 μM CTAC, the 300 mM NaCl system then displays a sharp increase in the SFG E-field and reaches a maximum constant level at 40 μM CTAC. In contrast, the 10 mM NaCl system reaches maximum SFG E-field at concentrations above 60 μM CTAC.

The data in Figure 7B suggests that the surfactant adlayer structure becomes more ordered with increasing surface coverage when in the presence of high (300 mM NaCl) ionic strengths. For instance, at low concentrations, surfactant molecules may be adsorbed as individual monomers with headgroups that sample a wide range of molecular orientations and tails that are likely to curl up to minimize unfavorable water−hydrocarbon interactions, as reported by Roke et al. and Miranda et al.[53,54] Such highly disordered structures would result in weak SFG responses. With increasing surfactant concentrations, the system is likely to transition from adsorbed monomers to aggregates, such as adsorbed micelles, producing a sharp increase in the SFG response that scales nonlinearly with adsorbate surface density. Given the low contact angles measured for CTAC-laden droplets on glass (see Supporting Information), we rule out the possibility of the presence of a hydrophobic surfactant monolayer. Adsorbed micelles are expected to have a stronger SFG response than disordered, adsorbed monomers because the surfactant headgroups pointed toward aqueous phase are not equivalent to the surfactant headgroups pointed toward the silica substrate, which corresponds to a noncentrosymmetric structure. Before reaching surface saturation, the adlayer may undergo further rearrangement, leading to the second "plateau" observed in the SFG data. Published AFM experiments[6] have identified both spherical micelles (0.1 mM CTAC, 100 mM NaCl) and elongated, rod-like micelles (6.4 mM CTAC, 3 M NaCl) at the silica/water interface (pH $\sim$6) for CTAC and NaCl concentrations that span those used in our work. Thus, it is possible that this latter rearrangement is due to a subtle change of adsorbed micelle shape or surfactant packing within adsorbed micelles that is difficult to identify using SFG and SHG and warrants further investigation by other experimental work as well as theory.

The conclusions made here about surfactant aggregate structure in the presence of 10 and 300 mM NaCl are consistent with previously published work and current understanding of surfactant adsorption. For silica/water interfaces in the absence of added electrolyte and at circum-neutral and basic pH values (i.e., pH = 9.6), AFM and SFG studies have demonstrated that adsorbed CTAB forms micelle-like aggregates at concentrations considerably lower than surface saturation and the CMC.[13,25] While run at a different ionic strength (10 mM NaCl) and under more basic conditions (pH 11), our SFG experiments indicate that CTAC aggregates at interfaces at low surface coverage levels that are comparable to this previous work. Our conclusion that CTAC forms aggregates at 300 mM NaCl and high surface coverage agrees with previously published AFM experiments that observed micelle-like aggregates in the presence of 250 mM LiCl and circum-neutral pH values.[49] There is less supporting evidence for our conclusion that at 300 mM NaCl and low surface coverage disordered monomers are the primary adsorbed species. However, this result is consistent with the notion that Na^+ ions can compete with cationic surfactants for silica binding sites, thereby, reducing the number of adsorbed surfactant molecules and limiting the hydrophobic interactions that drive surfactant aggregation.[55] This competition is particularly important at low surfactant concentrations, where the Na^+ ion concentration is 4 orders of magnitude larger than the surfactant concentration and the silica surface retains its overall negative charge, which leads to favorable electrostatic interactions between the surface and positively charged adsorbates.[55] Future studies may provide further insight into the exact structure of CTAC across a range of surfactant and NaCl concentrations through the used of complementary approaches (e.g., the analysis of stretching frequencies in FTIR spectra, etc.).

VI. Conclusions

Utilizing SFG, we characterized how the structure of adsorbed CTAC at the fused silica/aqueous interface depends on surfactant concentration and ionic strength under basic conditions (pH or pD 11). Specifically, spectra were collected in the C−H stretching region for CTAC at low ionic strengths (10 mM NaCl) and high ionic strengths (300 mM NaCl). Signal contributions from the vibrational resonances of D_2O, the solvent, can be clearly observed at low ionic strengths when excess charge accumulates at the interface. However, at high ionic strengths the SFG spectra display no water resonances across a range of CTAC concentrations. This result suggests that adsorbed surfactant in the presence of high ionic strengths disrupts the water structure at fused silica/aqueous interfaces even when the interface is positively charged[14] from the presence of surface-bound surfactant near surface saturation.

To track ordering in the surfactant adlayer with increasing ionic strength, we compared the SFG intensities of the methylene peaks corresponding to the surfactant hydrocarbon backbone to the methyl peaks corresponding to the ammonium headgroup. The d^-/r^-_{HG} and d^+/r^-_{HG} ratios decrease with increasing ionic strength, which indicates that fewer *gauche* defects occur in the hydrocarbon backbone at higher ionic strengths. This increase in ordering likely results from more efficient packing

of surfactant molecules that undergo reduced Coulombic repulsion between headgroups due to counterion binding to the adlayer and nonspecific charge screening.

Lastly, to further understand the structure of the CTAC adlayer, the vibrational signatures of the headgroup were probed as a function of surfactant surface coverage. For low ionic strengths the resonant SFG E-field of the methyl asymmetric stretch tracks the surfactant surface coverage, indicating that molecular rearrangement does not occur. Instead, we conclude that CTAC aggregates adsorb to the silica/aqueous interface as spherical micelle-like structures at concentrations considerably lower than surface saturation and the CMC (i.e., at concentrations as low as $\sim 0.1 \times$ CMC, which corresponds to $\sim$40% of surface saturation). A very different concentration dependence is observed at high ionic strengths (300 mM NaCl). The SFG E-field of the asymmetric methyl stretch is not directly proportional to surface coverage and it deviates in a manner that suggests the presence of disordered adsorbed monomers at low CTAC concentrations (below 30 μM) and then the presence of adsorbed micelles at higher concentrations. The exact structures of the adsorbed surfactant aggregates at high ionic strengths are still not known. In future work, sophisticated orientation analysis using polarization resolved SFG measurements[31,56] could be combined with other techniques such as AFM[6,9] to shed further light on this difficult problem. In addition, heterodyne-detected SFG could be used to probe adsorbed surfactant structure at substantially lower surface coverage than studied here using conventional homodyne SFG.[57]

Acknowledgment. P.L.H. acknowledges support from Schlumberger and is an ARCS (Achievement Rewards for College Scientists) Foundation, Inc. Scholar, Chicago Chapter. We acknowledge Spectra-Physics Lasers, a division of Newport Corporation, for equipment support. We also acknowledge the International Institute for Nanotechnology (IIN) at Northwestern University for capital equipment support. F.M.G. is an Alfred P. Sloan Fellow.

Supporting Information Available: Theoretical description of the Eisenthal $\chi^{(3)}$ technique, which was used to determine the relative surfactant surface coverage. Also included are the experimental results for determining the CTA CMC from interfacial tension measurements. Contact angle measurements for surfactant-laden drops on glass are provided for 10, 100, 300, and 500 mM NaCl concentrations, along with a discussion of autophobing. This material is available free of charge via the Internet at http://pubs.acs.org.

References and Notes

(1) Chase, B.; Chmilowski, W.; Marcinew, R.; Mitchell, C.; Dang, Y.; Krauss, K.; Nelson, E.; Lantz, T.; Parham, C.; Plummer, J. *Oilfield Rev.* **1997**, *9*, 20.
(2) Sau, T. K.; Murphy, C. J. *Langmuir* **2005**, *21*, 2923.
(3) Atkin, R.; Craig, V. S. J.; Wanless, E. J.; Biggs, S. *Adv. Colloid Interface Sci.* **2003**, *103*, 219.
(4) Paria, S.; Khilar, K. C. *Adv. Colloid Interface Sci.* **2004**, *110*, 75.
(5) Gu, T.; Huang, Z. *Colloids Surf.* **1989**, *40*, 71.
(6) Velegol, S. B.; Fleming, B. D.; Biggs, S.; Wanless, E. J.; Tilton, R. D. *Langmuir* **2000**, *16*, 2548.
(7) Howard, S. C.; Craig, V. S. J. *Soft Matter* **2009**, *5*, 3061.
(8) Eskilsson, K.; Yaminsky, V. V. *Langmuir* **1998**, *14*, 2444.
(9) Hodges, C.; Biggs, S. *Adv. Powder Technol.* **2007**, *18*, 615.
(10) Gutig, C.; Grady, B. P.; Striolo, A. *Langmuir* **2008**, *24*, 13814.
(11) Gutig, C.; Grady, B. P.; Striolo, A. *Langmuir* **2008**, *24*, 4806.
(12) Fragneto, G.; Thomas, R. K.; Rennie, A. R.; Penfold, J. *Langmuir* **1996**, *12*, 6036.
(13) Tyrode, E.; Rutland, M. W.; Bain, C. D. *J. Am. Chem. Soc.* **2008**, *130*, 17434.
(14) Hayes, P. L.; Chen, E. H.; Achtyl, J. L.; Geiger, F. M. *J. Phys. Chem. A* **2009**, *113*, 4269.
(15) Boyd, R. W. *Nonlinear Optics*, 2nd ed.; Academic Press: New York, 2003.
(16) Shen, Y. R. *The Principles of Nonlinear Optics*; John Wiley & Sons: New York, 1984.
(17) Liu, J.; Conboy, J. C. *J. Am. Chem. Soc.* **2004**, *126*, 8376.
(18) Conboy, J. C.; Messmer, M. C.; Richmond, G. L. *Langmuir* **1998**, *14*, 6722.
(19) Esenturk, O.; Walker, R. A. *J. Chem. Phys.* **2006**, *125*, 174701.
(20) Imae, T.; Ikeda, S. *Colloid. Polym. Sci.* **1987**, *265*, 1090.
(21) Langmuir, D. *Aqueous Environmental Geochemistry*; Prentice-Hall, Inc: NJ, 1997.
(22) Stumm, W.; Morgan, J. J. Aquatic Chemistry. *Chemical Equilibria and Rates in Natural Waters*, 3rd ed.; John Wiley & Sons: New York, 1996.
(23) Lindman, B.; Puyal, M. C.; Kamenka, N.; Rymden, R.; Stilbs, P. *J. Phys. Chem.* **1984**, *88*, 5048.
(24) Howard, S. C.; Atkin, R.; Craig, V. S. J. *Colloids Surf., A* **2009**, *347*, 109.
(25) Fleming, B. D.; Biggs, S.; Wanless, E. J. *J. Phys. Chem. B* **2001**, *105*, 9537.
(26) Geiger, F. M. *Annu. Rev. Phys. Chem.* **2009**, *60*, 61.
(27) Shen, Y. R.; Ostroverkhov, V. *Chem. Rev.* **2006**, *106*, 1140.
(28) Richmond, G. L. *Chem. Rev.* **2002**, *102*, 2693.
(29) Gopalakrishnan, S.; Liu, D.; Allen, H. C.; Kuo, M.; Shultz, M. J. *Chem. Rev.* **2006**, *106*, 1155.
(30) Esenturk, O.; Walker, R. A. *J. Phys. Chem. B* **2004**, *108*, 10631.
(31) Wang, H.-F.; Gan, W.; Lu, R.; Rao, Y.; Wu, B.-H. *Int. Rev. Phys. Chem.* **2005**, *24*, 191.
(32) Weeraman, C.; Yatawara, A. K.; Bordenyuk, A. N.; Benderskii, A. V. *J. Am. Chem. Soc.* **2006**, *128*, 14244.
(33) Ong, S.; Zhao, X.; Eisenthal, K. B. *Chem. Phys. Lett.* **1992**, *191*, 327.
(34) Hayes, P. L.; Malin, J. N.; Konek, C. T.; Geiger, F. M. *J. Phys. Chem. A* **2008**, *112*, 660.
(35) Malin, J. N.; Hayes, P. L.; Geiger, F. M. *J. Phys. Chem. C* **2009**, *113*, 2041.
(36) Salafsky, J. S.; Eisenthal, K. B. *J. Phys. Chem. B* **2000**, *104*, 7752.
(37) Boman, F. C.; Gibbs-Davis, J. M.; Heckman, L. M.; Stepp, B. R.; Nguyen, S. T.; Geiger, F. M. *J. Am. Chem. Soc.* **2009**, *131*, 844.
(38) Boman, F. C.; Musorrafiti, M. J.; Gibbs, J. M.; Stepp, B. R.; Salazar, A. M.; Nguyen, S. T.; Geiger, F. M. *J. Am. Chem. Soc.* **2005**, *127*, 15368.
(39) Yan, E. C. Y.; Liu, Y.; Eisenthal, K. B. *J. Phys. Chem. B* **1998**, *102*, 6331.
(40) Zhao, X.; Ong, S.; Wang, H.; Eisenthal, K. B. *Chem. Phys. Lett.* **1993**, *214*, 203.
(41) Wang, J.; Chen, C.; Buck, S. M.; Chen, Z. *J. Phys. Chem. B* **2001**, *105*, 12118.
(42) Stokes, G. Y.; Gibbs-Davis, J. M.; Boman, F. C.; Stepp, B. R.; Condie, A. G.; Nguyen, S. T.; Geiger, F. M. *J. Am. Chem. Soc.* **2007**, *129*, 7492.
(43) Voges, A. B.; Al-Abadleh, H. A.; Musorrafiti, M. J.; Bertin, P. A.; Nguyen, S. T.; Geiger, F. M. *J. Phys. Chem. B* **2004**, *108*, 18675.
(44) Adamson, A. W. *Physical Chemistry of Surfaces*, 5th ed.; John Wiley & Sons: New York, 1990.
(45) Eftekhari-Bafrooei, A.; Borguet, E. *J. Am. Chem. Soc.* **2009**, *131*, 12034.
(46) Shaw, S. K.; Lagutchev, A.; Dlott, D. D.; Gewirth, A. A. *Anal. Chem.* **2009**, *81*, 1154.
(47) Bordenyuk, A. N.; Benderskii, A. V. *J. Chem. Phys.* **2005**, *122*, 134713.
(48) Jena, K. C.; Hore, D. K. *J. Phys. Chem. C* **2009**, *113*, 15364.
(49) Subramanian, V.; Ducker, W. A. *Langmuir* **2000**, *16*, 4447.
(50) Atkin, R.; Craig, V. S. J.; Wanless, E. J.; Biggs, S. *J. Colloid Interface Sci.* **2003**, *266*, 236.
(51) Israelachvili, J. N.; Mitchell, D. J.; Ninham, B. W. *Biochim. Biophys. Acta, Biomembr.* **1977**, *470*, 185.
(52) Wampler, R. D.; Moad, A. J.; Moad, C. W.; Heiland, R.; Simpson, G. J. *Acc. Chem. Res.* **2007**, *40*, 953.
(53) Roke, S.; Schins, J.; Muller, M.; Bonn, M. *Phys. Rev. Lett.* **2003**, *90*, 128101.
(54) Miranda, P. B.; Shen, Y. R. *J. Phys. Chem. B* **1999**, *103*, 3292.
(55) Atkin, R.; Craig, V. S. J.; Biggs, S. *Langmuir* **2001**, *17*, 6155.
(56) Chen, X.; Wang, J.; Boughton, A. P.; Kristalyn, C. B.; Chen, Z. *J. Am. Chem. Soc.* **2007**, *129*, 1420.
(57) Stiopkin, I. V.; Jayathilake, H. D.; Bordenyuk, A. N.; Benderskii, A. V. *J. Am. Chem. Soc.* **2008**, *130*, 2271.

JP911116Q